Functional inhibitory control dynamics in impulse control disorders in Parkinson's disease

Paz-Alonso PM, PhD,[1*] Navalpotro-Gomez I, MD,[2,3,4*] Boddy P, MSc,[1] Dacosta R, PhD,[2,3] Delgado-Alvarado M, MD, PhD,[2,3,5,6,7] Quiroga-Varela A, PhD,[2,3,8],Jimenez-Urbieta H, MSc,[2,3] Carreiras M, PhD,[1,9] and Rodriguez-Oroz MC, MD,PhD,[1,3,8,9,10]

[1]BCBL. Basque Center on Cognition, Brain and Language, Donostia-San Sebastián, Spain

[2]Neurodegenerative Disorders Area, Biodonostia Health Research Institute, Donostia-San Sebastián, Spain

[3]CIBERNED. Network Center for Biomedical Research in Neurodegenerative Diseases, Madrid, Spain

[4]Servei de Neurologia, Hospital del Mar, Parc de Salut Mar-IMIM, Barcelona, Spain

[5]Neurology Department, Sierrallana Hospital, Torrelavega, Spain

[6]IDIVAL, Valdecilla Biomedical Research Institute, Santander, Spain

[7]Biomedical Research Networking Center for Mental Health (CIBERSAM), Madrid Spain

[8]Neuroscience Area, Center for Applied Medical Research (CIMA), Universidad de Navarra, Pamplona, Spain

[9]Ikerbasque (Basque Foundation for Science), Bilbao, Spain

[10]Department of Neurology, Clínica Universidad de Navarra, Universidad de Navarra, Pamplona, Spain

*P.M.P-A and I.N-G contributed equally to this work as joint first authors.

Corresponding authors: Maria C Rodriguez-Oroz, Department of Neurology, Clinica Universidad de Navarra, Universidad de Navarra, Pamplona, Spain. Phone: +34948255400 Ext: 4511; E-mail address: mcroroz@unav.es. Pedro M. Paz-Alonso,

BCBL, Basque Center on Cognition, Brain and Language, Donostia-San Sebastián, Spain. Phone: +34943300309; E-mail address: ppazalonso@bcbl.eu.

Key words: Parkinson´s disease, impulse control disorders, reward processing, inhibitory control, ventral striatum

ABSTRACT

- **Background:** Impulse control disorders (ICD) related to alterations in the mesocorticolimbic dopamine network occur in Parkinson's disease (PD). Our objective is to investigate the functional neural substrates of reward processing and inhibitory control in these patients.
- **Methods:** Eighteen PD patients with ICD, 17 without this complication, and 18 healthy controls, performed a version of the Iowa Gambling Task during functional magnetic resonance scanning under three conditions: positive, negative and mixed feedback. Whole-brain contrasts, regions-of-interest, time courses, functional connectivity analyses and brain-behavior associations were examined.
- **Results:** PD patients with ICD exhibited hyperactivation in subcortical and cortical regions typically associated with reward processing and inhibitory control compared to their PD and healthy control counterparts. Time course analyses revealed that only PD patients with ICD exhibited stronger signal intensity during the initial versus final periods of the negative feedback condition in bilateral insula, and right ventral striatum. Interestingly, hyperactivation of all the examined right-lateralized fronto-striatal areas during negative feedback was positively associated with ICD severity. Importantly, positive associations between ICD severity and regional activations in right insula and right inferior frontal gyrus, but not right subthalamic nucleus, were mediated by functional connectivity with right ventral striatum.
- **Conclusions:** During a reward-based task, PD patients with ICD showed hyperactivation in a right-lateralized network of regions, including the subthalamic nucleus that was strongly associated with ICD severity. In these patients, the right ventral striatum in particular, play a critical role in modulating the functional dynamics of right-lateralized inhibitory-control frontal regions when facing penalties.

1. INTRODUCTION

Impulse control disorders (ICD), including pathological gambling, binge eating, compulsive shopping, hypersexuality and other impulsive-compulsive behaviors (ICBs) are reported to occur at least in 13.6% of patients with Parkinson disease (PD) on dopaminergic medication[1,2]. Importantly, ICD can result in devastating financial, legal, or psychosocial problems[3].

Although the neuropathophysiological basis of ICD in PD patients is not well understood, it has been hypothesized to occur as a result of chronic administration of dopaminergic drugs, which modulate the reward network in PD patients[4]. Confirming the role of dopamine as a reinforcement signal shaping future motivated behaviors, positron emission tomography studies focused on the dopaminergic system indicate that ICDs in PD are associated with a higher release of dopamine in the ventral striatum (VS) during reward-related tasks[5,6]. However, functional magnetic resonance imaging (fMRI) studies using reward-related tasks in PD patients with ICD (PD-ICD) show discrepant results: while two studies pointed towards diminished activation in right VS, orbitofrontal (OFC) and anterior cingulate cortices (ACC)[7,8], three other studies showed higher activation in VS, anterior prefrontal cortex (PFC), ACC, and OFC[9–11]. These discrepancies could be due to methodological factors, such as clinical differences in the PD populations studied (e.g., PD severity, ICD subtype, with or without treatment), the use of different reward-related tasks (e.g., related or not to a specific ICD subtype), MRI imaging protocols and analytical approaches. Moreover, while few studies have investigated functional connectivity (FC) during incentive-based tasks in PD-ICD patients[12,13], the limited evidence available indicates mesolimbic pathway alterations and suggests ICD in PD patients reflect disruptions beyond this pathway.

In addition, studies of PD-ICD patients highlight a critical imbalance between learning from rewards and penalties[14], suggesting that chronic dopaminergic treatment might cause tonic stimulation of dopamine receptors, desensitizing the dopaminergic reward system by preventing the decreases in dopaminergic transmission that normally occur with penalties[15]. Furthermore, previous evidence has revealed that, in PD patients with or without ICD, dopaminergic drugs respectively decrease or increase activity in brain areas implicated in inhibitory control[16], classically strongly lateralized to the right hemisphere[17]. In this sense, the Iowa Gambling Task (IGT) is a useful experimental paradigm extensively used in clinical research to examine reward-related and inhibitory control processes in a decision-making context simulating real-life situations that has not been previously used with fMRI to examine the functional dynamics of reward and inhibitory control processes in PD-ICD.

Previous fMRI studies with normal adults using the IGT provide evidence that areas related to reward processing and inhibitory control such as the middle frontal gyrus (MFG), insula, OFC, ventromedial PFC, VS, ACC and supplementary motor area (SMA) are involved in the execution of this task[18,19]. On the other hand, clinical studies evaluating the performance of the IGT have reported that PD patients may show higher losses[20] or, conversely, intact or even more cautious performance of the task[21,22], reflecting opposite motivational expressions along a continuous behavioral spectrum involving hypo- and hyper-dopaminergic symptoms[23]. Neuroanatomical correlates of studies using the IGT task with PD patients point towards an association with the volumetry of limbic cortical areas[24,25] or with the function of the limbic fronto-striatal circuit of the basal-ganglia[26]. Interestingly, behavioral studies that have assessed the IGT task in PD-ICD patients have also shown mixed findings[27,28], further underscoring

the need to investigate the neural dynamics of PD-ICD patients during reward-related and inhibitory control processes in a decision-making task such as the IGT.

Our aim is to investigate the neural mechanisms underlying decision-making and inhibitory control processes in PD-ICD patients while performing the IGT task using fMRI. Specifically, in this study we sought to examine whether the type of feedback and ICD severity affects regional activation and FC between regions along the mesocorticolimbic circuit in PD-ICD patients. We hypothesized that these patients, would exhibit differential functional activation and connectivity patterns involving regions belonging to the mesocorticolimbic circuit, specifically the VS, during their execution of decision making and inhibitory control processes required by the IGT.

2. MATERIAL AND METHODS.

2.1. Participants

The final study sample included 53 participants comprised of three groups: 18 PD-ICD patients, 17 PD patients without ICD symptoms (PD-noICD), and 18 healthy controls (HC). Participants in each group were matched on age, sex, education and premorbid Intelligence Quotient. All PD patients were diagnosed according to the UK Parkinson's Disease Society Brain Bank criteria and recruited from the Movement Disorders Unit of the Hospital Donostia (Spain). Inclusion criteria for the PD-ICD group included at least one current ICD that had emerged after PD diagnosis and the initiation of dopamine replacement therapy. Each patient was routinely asked about any abnormal behavior and both a neurologist and a psychiatrist assessed and confirmed the presence of ICD based on the Diagnostic and Statistical Manual of Mental Disorders research criteria and on the Questionnaire for Impulsive-Compulsive Disorders in PD[29]. ICD symptom severity was then evaluated via the Questionnaire for Impulsive-Compulsive Disorders

in Parkinson's Disease-Rating Scale (QUIP-RS)[30]. In addition, we also confirmed that every PD-ICD patient had a QUIP-RS score above the published cut-off for each ICD subtype. Exclusion criteria were dementia[31] or mild cognitive impairment according to the Movement Disorders Society Task Force criteria (Level II)[32], dyskinesias, brain surgery; and those ICD patients who were no longer symptomatic when examined were also excluded. HC were recruited from the Basque Center on Cognition, Brain and Language (BCBL) pool of participants. This study was approved by the Gipuzkoa Clinical Research Ethics Committee and written informed consent was obtained from all the subjects.

2.2. Demographic and clinical assessment

All assessments were performed using a comprehensive battery of motor, behavior and cognitive tests as described in Table 1 (Demographic and clinical characteristics) and in Supplementary Table 1 (Neuropsychological test scores). Details of each patient's ICD characteristics are provided in Supplementary Table 2. Decision-making was assessed using the computerized version of the classical IGT, in which patients have to choose between four decks of cards in an attempt to win as much money as possible, across five blocks of task trials[33]. They have to take into account that some decks (advantageous) will tend to reward the player more often that other decks (disadvantageous; see Supplementary Data for a full description of the classical IGT). Afterwards, this classical IGT was compared with participants' in-scanner performance on the modified version of the IGT used in the present fMRI study. Details on the statistical analyses conducted on the demographic and clinical data are described in Supplementary Data. All assessments as well as MRI scanning of PD patients was done in the morning while they were still under the effect of their first regular dose of dopaminergic medication.

Table 1. Demographic and clinical characteristics of the sample.

	PD-ICD n=18	PD-noICD n=17	HC n=18	*p*	Post-hoc (Bonferroni or U-Mann Whitney)
Age	62.3 (7.6)	61(8.7)	63 (9.7)	0.809[a]	
Sex, male (%)	16 (88.9%)	15 (88.2%)	15 (83.3%)	0.866[b]	
Education (years)	14.5 [9.8-18.5]	12 [10-17]	15 [9.5-20]	0.570[c]	
Premorbid IQ (WAIS-III Vocabulary)	46 [38.8-51.8]	49 [39-3.5]	50 [44.8-57.3]	0.193[c]	
Disease duration (years)	8 [5.1-10]	7 [4-10]	-	0.960[e]	
UPDRS-III	22.31 (6.6)	25.90 (8.2)	-	0.122[d]	
H&Y stage	2 [1.5-2.5]	2 [1.5-3]	-	0.492[b]	
$LEDD_{DA}$	261.7 (69.5)	211.8 (44.9)	-	0390[d]	
$LEDD_{TOTAL}$	940.6 (94.9)	841.4 (62.4)	-	0.455[d]	
HADS total	8.1 (7.3)	6.3 (2.8)	5.2 (3.2)	0.092[a]	
HADS-anxiety	4.9 (3.1)	3.5 (2.1)	4.3 (2.8)	0.412[a]	
HADS-depression	3.1 (2.4)	2.2(2.6)	1.9 (1.3)	0.145[a]	
QUIP-RS score	17 (7.5)	0.4 (0.7)	-	**<0.0001[d]**	
TCI-R Novelty Seeking total	100.5 (14.6)	84.8 (9.8)	84.4 (20.9)	**0.005[a]**	PD-ICD>PD-noICD (p=0.016) PD-ICD>HC (p=0.011)
NS1 Exploratory excitability	29.9 (7.2)	26.5 (3.8)	25.3 (5.3)	**0.045[a]**	PD-ICD>HC (p=0.049)
NS2 Impulsiveness	25.5 (6.7)	18.9 (3.4)	18.7 (5.5)	**0.002[a]**	PD-ICD>PD-noICD (p=0.003) PD-ICD>HC (p=0.003)
NS3 Extravagance	27.1 (4.3)	23.9 (3.5)	24.1 (5)	0.058[a]	
NS4 Disorderliness	17.8 (6.1)	14.5 (4)	15.3 (2.8)	0.248[a]	
Barratt Impulsiveness total	48.3 (11.7)	30.9 (8.4)	25.4 (8.2)	**<0.001[a]**	PD-ICD>PD-noICD (p=0.004) PD-ICD>HC (p=0.003)
Barratt Cognition	15.1 (4.6)	10.3 (3.8)	8.7 (3.3)	**0.004[a]**	PD-ICD>PD-noICD (p=0.012) PD-ICD>HC (p=0.004)
Barratt Motor Impulsivity	17.6 (6.4)	10.6 (4.5)	8.8 (4.4)	**0.001[a]**	PD-ICD>PD-noICD (p=0.013) PD-ICD>HC (p=0.001)
Barratt Non-planning	16.1 (9)	9.9 (3.2)	8 (4.8)	**0.001[a]**	PD-ICD>PD-noICD (p=0.016)
Starkstein score	6.6 (2.3)	3.5 (2.9)	1.9 (1.2)	**0.013[a]**	PD-ICD>HC (p=0.01)
Iowa Gambling Task outside scanner (CD *minus* AB, %)	39.2 (12.4)	41.3 (23.4)	43.7 (27.7)	0.113[f]	
Modified Iowa Gambling-Task in-scanner (No-risk *minus* risk, %)	26.8 (18.1)	35.4 (12.5)	38.9 (29.9)	0.548[f]	

Values expressed in mean (SD) for parametric variables, in median and IQ range in non-parametric variables

[a] One factorANOVA; [b] Chi-Square; [c] Kruskall-Wallis; [d] Two-sample T-test; [e] U Mann Whitney; [f] Repeated measures ANOVA

Abbreviations: IQ = Intelligence Quotient; WAIS-III = Wechsler Adult Intelligence Scale-III; UPDRS = Unified Parkinson's Disease Rating Scale; H&Y=Hoehn and Yahr scale; $LEDD_{DA}$: levodopa equivalent daily dose of dopamine agonist was calculated using the formula described by Tomlinson et al. (Tomlinson et al., 2010); $LEDD_{TOTAL}$= Total levodopa equivalent daily dose was calculated according to the same formula; HADS=Hospital Anxiety and Depression Scale; QUIP-RS= Questionnaire for Impulsive-Compulsive Disorders in Parkinson's Disease-Rating Scale; TCI-R=Revised Temperament and Character Inventory; NS=Novelty Seeking Subscales.

2.3. MRI data acquisition

Functional and structural images were obtained at the BCBL using a 3T Siemens Magnetom TIM Trio MRI scanner using a 32-channel head coil. See Supplemental data for further information on MRI data acquisition.

2.4. Functional magnetic resonance imaging paradigm

At the scanner participants performed a modified version of the IGT task. Before starting the IGT, participants were instructed that their aim was to gain as much money as possible. However, they were not informed about the IGT contingencies and had to learn them from feedback on their card choices, that is, their monetary gains and losses. The fMRI design conformed to a slow event-related design with gambling-related visual cues alternating with neutral stimuli.

We used a simplified version of the IGT to minimize motor difficulties experienced by PD patients during scanning and to assure that they could understand the IGT contingencies. Instead of the original version (with decks A, B, C and D), we used a version with only two decks (A and B). One of the decks was disadvantageous, providing larger gains but larger losses resulting in a net loss over time. The other deck was advantageous, providing smaller gains but smaller losses resulting in a net gain

over time. These deck contingencies were kept consistent across conditions (i.e., positive, negative and mixed), regardless of the feedback specifically provided in each of these conditions. The subject chose a card from either of the two decks, then a message was displayed on the screen indicating the amount of money the subject had won or lost. The task was divided into 3 conditions always presented in the same sequential order: (1) only positive feedback was presented, so the participants could get familiarized with the decks providing lower and higher gains (positive); (2) negative feedback was presented, so participants could get familiarized with the decks providing higher and lower losses (negative); and, (3) positive and negative rewards were provided, so participants could either win or lose money based on the contingencies learned in sections 1 and 2 (see Supplementary Data for a further description of the modified IGT used here). Participants performed this modified version of the IGT across three functional runs. Within each of these functional runs, participants performed two blocks, each including the three sequential sections (6 in total). Blocks presented within the same functional run differed from each other in regard to advantageous and disadvantageous rules applied, and participants were instructed to ignore previous contingencies when moving from one block to the next one. Between blocks participants performed a control task where they encountered two decks (A and B) with different amounts written on each deck and they just needed to choose the deck with the highest number.

2.5. MRI data analyses

To examine potential group differences in gray-matter surface we used participants' T1-weighted images to run Freesurfer's mri_glmfit. This analysis revealed no significant differences for any of the possible group comparisons.

Further details on the MRI data preprocessing and analyses are reported in Supplementary Data. In brief, SPM8 was used to conduct standard preprocessing routines and analyses. Statistical analyses were performed on individual participants' data using the general linear model (GLM). The fMRI time series data were modeled by a series of events convolved with a canonical hemodynamic response function. Four fMRI task experimental conditions were analyzed separately as epochs from the onset of the presentation of the first stimulus within each section (positive feedback, negative feedback, mixed feedback) and control task. The resulting functions were used as covariates in a GLM, along with the motion parameters for translation and rotation as covariates of non-interest. The model was created to examine the neural changes restricted to the three task sections and the control task periods and was used in whole-brain contrast, regions-of-interest (ROIs), time course and FC analyses. Additionally, brain-behavior associations with ICD severity in PD-ICD patients were examined for ROI and FC analyses. Finally, mediation analyses were conducted to examine whether in PD-ICD patients FC mediates the relation between ICD severity and regional activation (see Supplementary Data for details).

3. RESULTS

3.1.Demographic and clinical data

No differences were seen in demographic data, dopaminergic medication or clinical features with the exception of impulsivity scores that were significantly higher in PD-ICD patients than in PD-noICD patients and HC (Table 1 and Supplementary Table 1). There were 6 patients who reported a single 'isolated' ICD and 12 patients with 'combined' ICD/ICB (Supplementary Table 2).

3.2. In- and out-scanner IGT results

The ANOVA on the net scores of the classical IGT that participants performed outside of the scanner revealed no significant main effects of Group ($F(2, 50)=2.28$; $p=0.11$, $\eta_p^2=0.08$) and Condition ($F(2, 50)=1.61$; $p=0.18$, $\eta_p^2=0.08$), nor Group by Condition interaction ($F(2, 50) =1.51$; $p=0.20$, $\eta_p^2=0.05$). The results on the modified in-scanner IGT task resembled the results obtained with the classical IGT (Supplementary Fig.1). We also compared classical IGT task results with modified in-scanner IGT task results revealing no differences between both task performance ($F(2, 50)=1.02$; $p=0.366$, $\eta_p^2=0.04$).

3.3.MRI results

3.3.1. Whole-brain analysis

To identify brain regions involved in the in-scanner functional IGT task across all participants, we computed a whole-brain contrast for all the activation conditions versus the control condition (All Conditions > Control). This contrast revealed activation in fronto-parietal networks, including bilateral inferior and superior parietal cortex and bilateral inferior, middle and superior PFC[18]. Also, significant engagement of bilateral insula, OFC, VS and right STN were shown in this contrast.

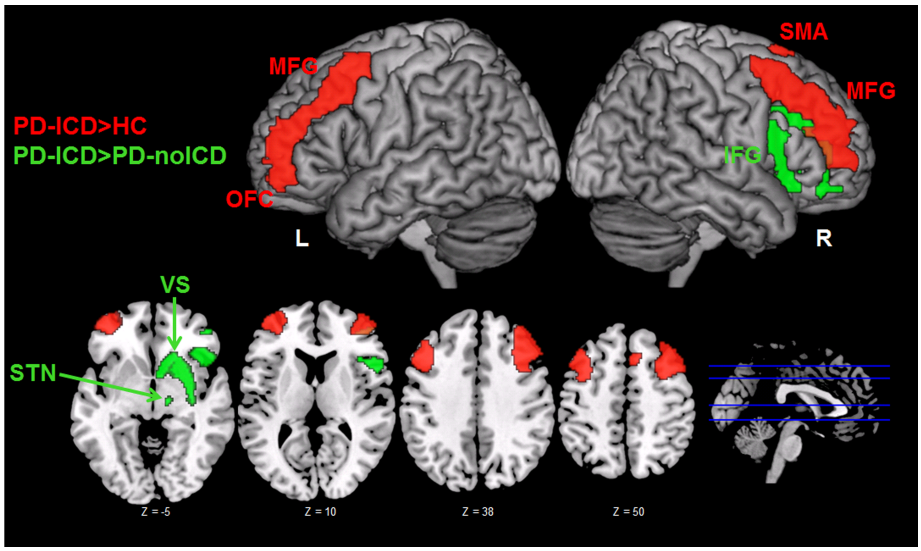

Figure 1 Brain rendering and axial sections showing ROI analyses that revealed main group effects in % signal change. In red are shown regions with stronger activation for the PD-ICD group compared to the HC group. Regions in green showed higher activation for the PD-ICD group compared to the PD-noICD group. MFG = Middle frontal gyrus; OFC = orbitofrontal cortex; SMA = supplementary motor area; IFG = inferior frontal gyrus; STN = subthalamic nucleus; VS = ventral striatum.

3.3.2. ROI analysis

ROI analysis showed stronger regional activation in PD-ICD patients compared with HC across the 3 conditions of the IGT in the following regions (areas in red in Fig.1): left MFG ($F(2, 49)=5.84$; $p=0.005$, $\eta_p^2=0.19$), left medial OFC ($F(2, 50)=3.81$; $p=0.03$, $\eta_p^2=0.13$), right MFG ($F(2, 49)=2.69$; $p=0.03$, $\eta_p^2=0.14$) and right SMA ($F(2, 50)=4.43$; $p=0.017$, $\eta_p^2=0.15$). Group effects in these regions were not observed for PD-ICD versus PD-noICD.

ROI analysis also showed hyperactivation in PD-ICD patients compared to PD-noICD patients across the 3 conditions of the IGT in the following regions (areas in green in Fig.1): right STN ($F(2, 49)=3.36$; $p=0.04$, $\eta_p^2=0.12$), right IFG ($F(2, 50)=3.38$; $p=0.04$, $\eta_p^2=0.12$), and right VS ($F(2, 50)=3.58$; $p=0.03$, $\eta_p^2=0.13$). Moreover, PD-noICD patients showed hypoactivation compared to HC only in bilateral dorsal striatum ($Fs(2, 50)=3.19$; $ps\leq0.04$, $\eta_p^2\geq0.12$).

3.3.3. Time-course analysis

The ANOVA conducted on the BOLD signal intensity extracted from time-course analyses in each ROI revealed a Group X Condition X Time interaction in the left insula

(F(2,50)=1.7; p=0.01, η_p^2=0.264), right insula (F(2, 50)=1.72; p=0.01, η_p^2=0.25) and right VS (F(2, 50)=1.48; p=0.04, η_p^2=0.16). Post-hoc analyses in all three regions revealed that only PD-ICD patients exhibited significantly higher signal intensity during the negative feedback condition in the initial bin of the period (0-8 secs) compared to the second bin of the period (8-16 secs) in the left insula (F(2, 18)=6.7; p=0.003, η_p^2=0.45), right insula (F(2, 18)=7.2; p=0.002, η_p^2=0.30) and right VS (F(2, 18)=5.3; p=0.01, η_p^2=0.24) (Fig.2). These effects were not observed in PD-noICD patients, or in HC (ps≥0.09).

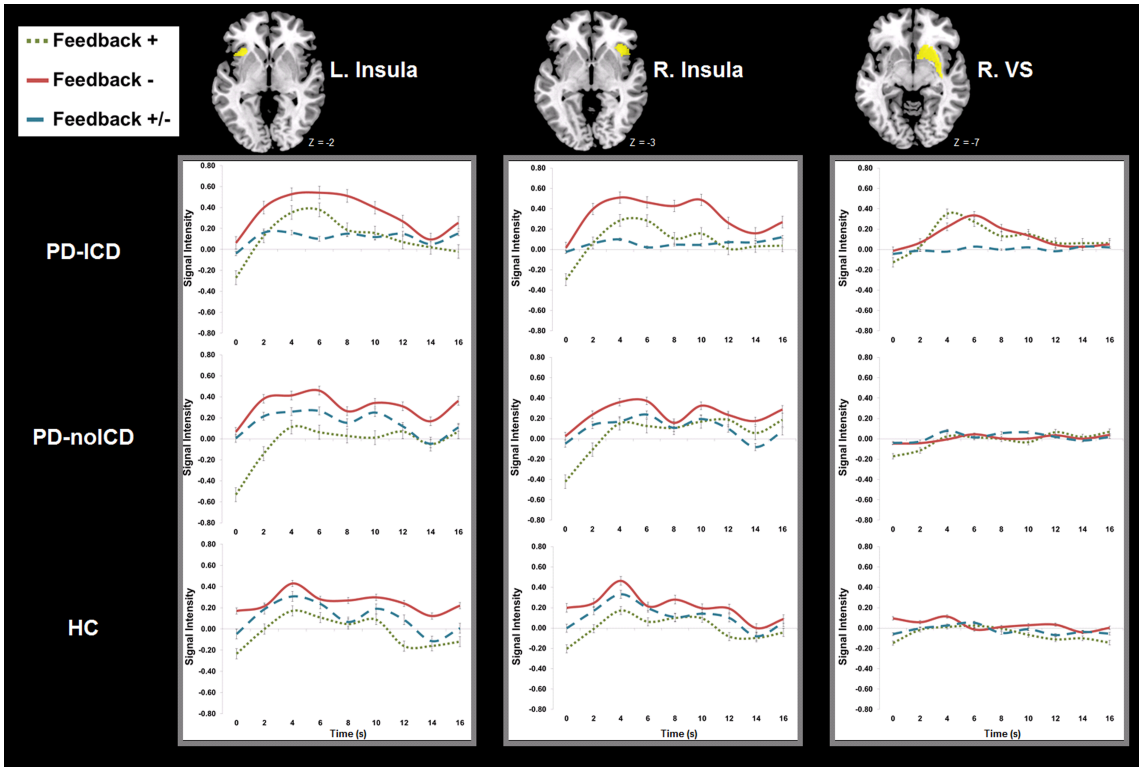

Figure 2 Time-course analysis of ROIs (in axial sections) showing a Group X Condition X Time interaction: bilateral insula and right VS. All these regions demonstrated larger BOLD signal intensity in the negative feedback condition for the PD-ICD group during the initial period relative to the PD-noICD and HC groups. This effect was not present in the final period. L. = Left; R. = Right; VS = ventral striatum.

3.3.4. QUIP correlates, functional connectivity, and mediation analysis

In PD-ICD patients, positive associations were found between regional activation during negative feedback and QUIP-RS scores for some of the right-lateralized ROIs: STN (r(16)=0.75; q=0.001), MFG (r(16)=0.50; q=0.02), IFG (r(16)=0.53; q=0.02), SMA (r(16)=0.50; q=0.02), insula (r(16)=0.52; q=0.02) and VS (r(16)=0.62; q=0.01).

To examine if the association between regional activation during the negative feedback condition and ICD severity was mediated by specific patterns of FC among these areas, we first examined whether pairwise FC among the above mentioned six right-lateralized ROIs was associated with ICD severity (Fig.3A). FC during the negative feedback condition among 4 of these six areas (i.e., STN, VS, IFG and insula) was associated with ICD severity: VS-STN (r(16)=0.77; q=0.001), VS-insula (r(16)=0.75; q=0.001), and VS-IFG (r(16)=0.50; q=0.048).

Mediation analyses (Fig.3B) revealed that 1) the FC strength between VS-Insula mediated the association between ICD severity and right insula regional activation (F(2, 17)=10.28, p=0.002); and, 2) connectivity between VS-IFG mediated the association between ICD severity and right IFG regional activation (F(2, 17)=9.52, p=0.002).

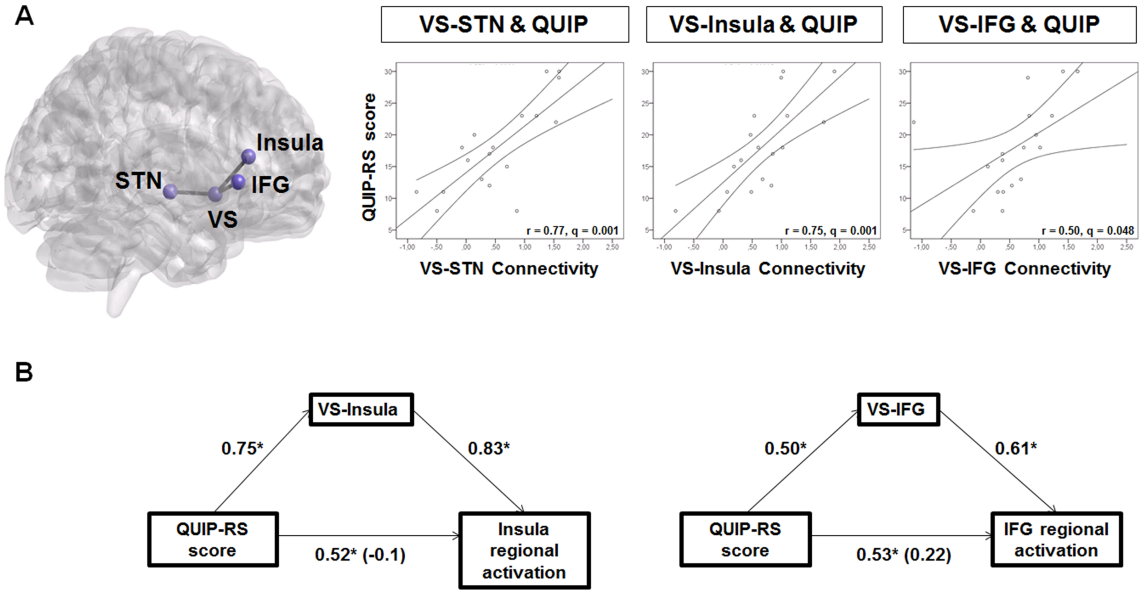

Figure 3 (A) Right brain rendering including pairs of nodes (VS-STN, VS-IFG, VS-Insula) that showed significant positive associations between the functional connectivity among them during the negative feedback condition and ICD severity (QUIP-RS). (B) Mediation analyses revealing that positive associations between ICD severity and regional activation of right insula and right IFG during negative feedback were mediated by the functional connectivity of these respective regions with the right VS. STN = subthalamic nucleus; VS = ventral striatum; IFG = inferior frontal gyrus.

4. DISCUSION

Based on previous evidence, we postulated that PD-ICD patients would exhibit differential neural dynamics involving the mesocorticolimbic dopaminergic circuit during the execution of a reward-related task. This was in fact the case, and even where behavioral performance was equivalent, PD-ICD patients exhibited differential patterns of activation and FC compared to PD-noICD patients and HC. Compared to PD-noICD patients, PD-ICD patients showed hyperactivation that was restricted to the right-hemisphere cortical and subcortical regions associated with reward processing and inhibitory control. In fact, the higher the severity of ICD, the higher the regional activation of these areas, especially when patients were faced with penalties. Moreover, PD-ICD patients exhibited higher peaks in signal intensity during early processing of negative rewards in conflict detection areas, such as the insula; and reward processing regions, such as the right VS. A compelling finding was that functional coupling with right VS mediated the relation between ICD severity and the engagement of right-lateralized inhibitory control regions (insula, IFG) during negative rewards in PD-ICD patients. These observations demonstrate that inhibitory control regions in PD-ICD patients are modulated by the right VS, which appears to orchestrate reward-processing

dynamics when patients face penalties requiring inhibitory control. A novel finding of this study was the involvement of the right STN in this process. However, unlike insula and IFG, STN activity was not mediated by functional coupling with VS. Importantly, although previous works investigated motor inhibition in PD patients with and without ICD, this was the first study to investigate the neural correlates of reward and inhibitory control processes during a decision-making IGT in PD-ICD patients and the first to show the involvement of the STN in cognitive inhibitory control.

ICD in PD is a multidimensional concept engaging alterations in certain cognitive functions, such as reward processing, learning from reward and loss, inhibitory control, risk-taking and conflict processing[4]. In this regard, the IGT assesses patterns of decision-making under risk[34], which requires the integration of processes conducted by different neural systems related to inhibitory control, memory and to the limbic system[18]. Accordingly, it has been previously reported that a disruption of ventral fronto-striatal circuits in PD-ICD patients might result in a reduced ability to resist an immediate reward, despite long-term consequences, termed 'myopia for the future'[35]. Clinical studies examining IGT performance in PD patients with or without ICD have either reported impaired decision-making,[20,24,27] absence of differences[28,36] or even a conservative attitude in PD patients compared to HC[37]. Due to the aforementioned discrepancies, here we used an in-scanner modified IGT task and out-scanner classical IGT task, with both tasks showing lack of behavioral differences among the groups here examined in line with previous evidence[28,36,38]. Of interest, despite this equivalence in behavioral performance, important differences in functional regional activation were observed between groups and in terms of FC in the PD-ICD group.

PD-ICD patients exhibited hyperactivation of bilateral MFG, left OFC and right SMA when compared to HC. These results complement previous fMRI studies in PD-ICD

patients, which have underscored the critical role of the mesocorticolimbic cortical system, encompassing insular cortex, PFC and OFC[7,10]. In addition, lateral PFC, MFG and SMA are part of the same fronto-striatal pathway that exhibits an activation pattern associated with interference inhibition, inhibitory control and action cancellation[39,40]. In this sense, ICD in PD patients is a multifaceted construct, including choice impulsivity and impairments in goal-directed behavior[41], which have been shown to rely on different neural networks[42,43]. Compared to PD-noICD patients, PD-ICD patients showed stronger activation in right hemisphere subcortical areas (STN and VS) and in a cortical region strongly associated with inhibitory control: the IFG[44]. The involvement of the STN in impulsive behavior in PD has been widely investigated. Oscillatory activity recorded in the STN of PD patients treated with deep brain stimulation is modified during the execution of motor inhibition tasks[45–47] and during inhibition of inappropriate or habitual prepotent responses[48,49]. fMRI studies have also revealed that during motor inhibition tasks there is hyperactivation of the right STN in control subjects, which is functionally connected to the right IFG and right pre-SMA through the hyperdirect pathway[50]. The IFG and STN are considered key nodes in the motor inhibition network; their activity is interrelated and also correlates with the extent of inhibition exercised[51]. Moreover, PD-ICD patients exhibit higher power in low frequency oscillations that is coherent with the oscillatory activity recorded in the prefrontal cortex[52]. On the other hand, the VS plays a central role in the mesocorticolimbic incentive network enabling the behavior-reinforcing effects of rewarding activities. Indeed, it has been extensively found that the VS, mostly in the right hemisphere, is implicated in the physiopathology of ICD in PD patients, and in keeping with these results, increased activation in the right VS could be related to increased dopamine release consistent with previous neuroimaging data[5]. Finally, right

IFG has been classically involved in inhibitory control along with lateral PFC and SMA[44]. The stronger engagement of all these regions in PD-ICD patients could be determined by the dopaminergic overstimulation of the mesolimbic areas that occurs in these patients, leading them toward aberrant reward evaluation. Our results also open the door for further research and therapeutic interventions, especially in the right STN and right VS, both areas where activation can be modulated by deep brain stimulation.

Time-course analysis pointed towards higher early BOLD signal intensity during the processing of negative rewards in PD-ICD patients in bilateral insula and right VS. It is known that dopaminergic medications can influence cognitive processes in PD patients, and supporting evidence points towards impaired learning from negative feedback that in PD-ICD patients has been characterised by a VS critic model[4,53,54]. In the present study, PD-ICD group differences in processing negative rewards occurred at the neural level without showing a differential group effect on behavioural performance. By contrast, PD patients without this complication have been characterised by a dorsal actor model with higher learning rates from positive feedback[54]. Murine models have also endorsed this theory as nucleus accumbens D2 stimulation with dopamine agonists reduced ability to learn from negative feedback[15]. Our results showing earlier peaks when facing penalties in regions involved in conflict monitoring, such as the right insula[55], and in reward processing, such as the right VS[12], might underlie a differential processing of negative rewards in PD-ICD patients during initial prediction errors and evaluation of rewards that precedes the normal posterior course of activation. So, this initial activation peak may be necessary to adjust PD-ICD neural responses to process subsequent penalties in a reward-processing context. Future neuroimaging studies using tasks requiring more transient functional processing of negative rewards in PD-ICD

patients may lead to the identification of concomitant group differences at the neural and behavioral levels.

Regarding FC, we observed that right VS functional coupling mediates the relation between ICD severity and the engagement of regions involved in conflict evaluation processes (insula) and inhibitory control (IFG) during negative rewards in PD-ICD patients[56]. Thus, in this context the right VS appears to be a critical hub. Previous evidence has revealed altered striato-cortical connectivity in PD-ICD patients, showing controversial results such as, on the one hand, reduced connectivity between dorsal striatum and temporal and cingulate cortices[57], and, on the other hand, stronger connectivity between right VS and fronto-temporal cortical areas[12]. Our results suggest that the coupling of the right VS with these two regions may serve as a bridge for communication between the reward system and cognitive control areas resulting in higher activation of those inhibitory control regions.

It is remarkable that although the connectivity between STN and VS was positively correlated with ICD severity, the VS did not mediate the association between STN recruitment and ICD severity. Although it is hard to make further sense of a null effect, the STN seems to be specifically engaged in late response inhibitory processes as reflected by studies showing a correlation between STN activation and longer stop signal delays[58]. As our time-course analysis revealed that only PD-ICD patients showed different signal intensity in the initial periods after being presented with negative feedback, it could be that STN and IFG involvement would be greater in later phases. In fact, the STN-IFG pathway is more activated in the global inhibition[59] and late inhibition phases as has been observed after right STN lesions in PD patients[60]. Future neuroimaging research including both response and cognitive inhibitory tasks with PD-ICD patients could further disentangle these possibilities.

These findings should be considered in the context of several limitations. First, all patients in this study were on their regular medication; this was intentional as ICD is a complication to which dopaminergic medication is the main contributor. However, we ensured that both groups of patients were receiving similar daily doses of antiparkinsonian medication to avoid any pharmacological confound. Second, as our sample was heterogeneous because of mixed ICD types, we decided to choose a global reward (an economic reward) and interpreted the results on this basis. Also for this reason, we tried not to choose PD-ICD patients with problems in only one ICD modality to avoid introducing a bias and because based on previous evidence it is reasonable to assume that the neural substrates in PD-ICD patients are similar for all modalities.

The theoretical and neurological framework presented here suggests that PD-ICD patients have enhanced activation in regions involved in the encoding of rewards and inhibitory control during disadvantageous outcomes, compared with PD-noICD and healthy controls. PD-ICD patients show hyperactivation during stimuli evaluation, conflict detection and monitoring areas during the early processing of negative rewards. In addition, in these patients, right VS appears to be a critical region that orchestrates hyperactivation in right-lateralized inhibitory-control frontal regions when facing penalties. Interestingly, the right STN is also a relevant area for cognitive inhibitory control although its activation is not modulated by the right VS. Importantly, although we found no group differences in behavioral performance, the neural dynamics in PD-ICD patients were different to those in PD-noICD patients and HCs, providing new insights into the investigation of neural functional alterations in these patients.

Authors´contributions

(1) Research project: A, Conception; B, Organization; C, Execution.

(2) Statistical analysis: A, Design; B, Execution; C, review and Critique

(3) Manuscript Preparation: A, Writing of the first draft; B, Review and Critique

P.M.P.-A.: 1A, 1B, 1C, 2A, 2B, 2C, 3A

I.N.-G.: 1A, 1B, 1C, 2A, 2B, 2C, 3A

P.B.: 1B, 1C, 2C, 3B

R.D.:1B, 1C, 2C, 3B

M.D.-A.: 2C, 3B

H.J.-U.: 2C, 3B

A.Q.-V.: 2C, 3B

J.R.-M.: 1C, 2C, 3B

A.B.-Y.: 1C, 2C, 3B

M.C.: 1A, 1B, 2C, 3B

M.C.R.-O.: 1A, 1B, 1C, 2C, 3B

Financial disclosures

Conflict of interest: Dr Rodriguez-Oroz received honoraria for lectures, travel and accommodation to attend scientific meetings from Zambon, Bial and Boston Scientific. Dr Navalpotro-Gomez received honoraria for travel and accommodation to attend scientific meetings from Zambon. Dr Delgado-Alvarado received honoraria for travel and accommodation to attend scientific meetings from UCB and Zambon. None of these funding bodies influenced the content of the manuscript or the decision to publish in any way.

Funding sources: This study was funded by the Carlos III Institute of Health (PI11/02109) and by the ERA-Neuron program (PIM2010ERN-00733). In addition, P.M.P-A. was supported by grants from the Spanish Ministry of Economy and Competitiveness (MINECO, RYC-2014-15440, PGC2018-093408-B-I00, SEV-2015-049), and the Diputación Foral de Gipuzkoa (OF301/2018). I.N-G. was the recipient of a Rio Hortega 2016 grant (CM16/00033) from the Carlos III Institute of Health. M.C.R-O. received financial support for her research from national and local government institutions in Spain (Institute of Health Carlos III, Basque Country Government, Diputacion Foral Guipuzcoa and CIBERNED).

REFERENCES

1. Weintraub D, Koester J, Potenza MN, et al. Impulse control disorders in Parkinson disease: a cross-sectional study of 3090 patients. Arch Neurol. 2010;67:589–595.

2. Weintraub D, Claassen DO. Impulse Control and Related Disorders in Parkinson's Disease. Int Rev Neurobiol. 2017;133:679–717.

3. Phu AL, Xu Z, Brakoulias V, et al. Effect of impulse control disorders on disability and quality of life in Parkinson's disease patients. J Clin Neurosci Off J Neurosurg Soc Australas. 2014;21:63–66.

4. Voon V, Napier TC, Frank MJ, et al. Impulse control disorders and levodopa-induced dyskinesias in Parkinson's disease: an update. Lancet Neurol. 2017;16:238–250.

5. O'Sullivan SS, Wu K, Politis M, et al. Cue-induced striatal dopamine release in Parkinson's disease-associated impulsive-compulsive behaviours. Brain. 2011;134:969–978.

6. Steeves TDL, Miyasaki J, Zurowski M, et al. Increased striatal dopamine release in Parkinsonian patients with pathological gambling: a [11C] raclopride PET study. Brain. 2009;132:1376–1385.

7. Voon V, Gao J, Brezing C, et al. Dopamine agonists and risk: impulse control disorders in Parkinson's; disease. Brain. 2011;134:1438–1446.

8. Rao H, Mamikonyan E, Detre JA, et al. Decreased ventral striatal activity with impulse control disorders in Parkinson's disease. Mov Disord. 2010;25:1660–1669.

9. Frosini D, Pesaresi I, Cosottini M, et al. Parkinson's disease and pathological gambling: results from a functional MRI study. Mov Disord Off J Mov Disord Soc. 2010;25:2449–2453.

10. Politis M, Loane C, Wu K, et al. Neural response to visual sexual cues in dopamine treatment-linked hypersexuality in Parkinson's disease. Brain. 2013;136:400–411.

11. Girard R, Obeso I, Thobois S, et al. Wait and you shall see: sexual delay discounting in hypersexual Parkinson's disease. Brain J Neurol. 2019;142:146–162.

12. Petersen K, Van Wouwe N, Stark A, et al. Ventral striatal network connectivity reflects reward learning and behavior in patients with Parkinson's disease. Hum Brain Mapp. Epub 2017 Oct 31.

13. Filip P, Linhartová P, Hlavatá P, et al. Disruption of Multiple Distinctive Neural Networks Associated With Impulse Control Disorder in Parkinson's Disease. Front Hum Neurosci. 2018;12:462.

14. Cilia R. How neurodegeneration, dopamine and maladaptive behavioral learning interact to produce impulse control disorders in Parkinson's disease. Basal Ganglia. 2012;2:195–199.

15. Goto Y, Grace AA. Dopaminergic modulation of limbic and cortical drive of nucleus accumbens in goal-directed behavior. Nat Neurosci. 2005;8:805–812.

16. Jahanshahi M, Obeso I, Rothwell JC, Obeso JA. A fronto–striato–subthalamic–pallidal network for goal-directed and habitual inhibition. Nat Rev Neurosci. 2015;16:719–732.

17. Garavan H, Ross TJ, Stein EA. Right hemispheric dominance of inhibitory control: an event-related functional MRI study. Proc Natl Acad Sci U S A. 1999;96:8301–8306.

18. Li X, Lu Z-L, D'Argembeau A, Ng M, Bechara A. The Iowa Gambling Task in fMRI images. Hum Brain Mapp. Epub 2009.:NA-NA.

19. Eckert MA, Menon V, Walczak A, et al. At the heart of the ventral attention system: the right anterior insula. Hum Brain Mapp. 2009;30:2530–2541.

20. Pagonabarraga J, García-Sánchez C, Llebaria G, Pascual-Sedano B, Gironell A, Kulisevsky J. Controlled study of decision-making and cognitive impairment in Parkinson's disease. Mov Disord Off J Mov Disord Soc. 2007;22:1430–1435.

21. Poletti M, Cavedini P, Bonuccelli U. Iowa gambling task in Parkinson's disease. J Clin Exp Neuropsychol. 2011;33:395–409.

22. Poewe W, Karamat E, Kemmler GW, Gerstenbrand F. The premorbid personality of patients with Parkinson's disease: a comparative study with healthy controls and patients with essential tremor. Adv Neurol. 1990;53:339–342.

23. Sierra M, Carnicella S, Strafella AP, et al. Apathy and Impulse Control Disorders: Yin & Yang of Dopamine Dependent Behaviors. Korczyn AD, Reichmann H, Chaudhuri KR, editors. J Park Dis. 2015;5:625–636.

24. Ibarretxe-Bilbao N, Junque C, Tolosa E, et al. Neuroanatomical correlates of impaired decision-making and facial emotion recognition in early Parkinson's disease. Eur J Neurosci. 2009;30:1162–1171.

25. Kobayakawa M, Tsuruya N, Kawamura M. Decision-making performance in Parkinson's disease correlates with lateral orbitofrontal volume. J Neurol Sci. 2017;372:232–238.

26. Gescheidt T, Czekóová K, Urbánek T, et al. Iowa Gambling Task in patients with early-onset Parkinson's disease: strategy analysis. Neurol Sci. 2012;33:1329–1335.

27. Rossi M, Gerschcovich ER, De Achaval D, et al. Decision-making in Parkinson's disease patients with and without pathological gambling: Decision-making in PD with pathological gambling. Eur J Neurol. 2010;17:97–102.

28. Biars JW, Johnson NL, Nespeca M, Busch RM, Kubu CS, Floden DP. Iowa Gambling Task Performance in Parkinson Disease Patients with Impulse Control Disorders. Arch Clin Neuropsychol Off J Natl Acad Neuropsychol. Epub 2018 Apr 27.

29. Weintraub D, Hoops S, Shea JA, et al. Validation of the questionnaire for impulsive-compulsive disorders in Parkinson's disease. Mov Disord Off J Mov Disord Soc. 2009;24:1461–1467.

30. Weintraub D, Mamikonyan E, Papay K, Shea JA, Xie SX, Siderowf A. Questionnaire for impulsive-compulsive disorders in Parkinson's Disease-Rating Scale. Mov Disord. 2012;27:242–247.

31. Emre M, Aarsland D, Brown R, et al. Clinical diagnostic criteria for dementia associated with Parkinson's disease. Mov Disord Off J Mov Disord Soc. 2007;22:1689–1707; quiz 1837.

32. Litvan I, Goldman JG, Tröster AI, et al. Diagnostic criteria for mild cognitive impairment in Parkinson's disease: Movement Disorder Society Task Force guidelines. Mov Disord Off J Mov Disord Soc. 2012;27:349–356.

33. Bechara A, Damasio AR, Damasio H, Anderson SW. Insensitivity to future consequences following damage to human prefrontal cortex. Cognition. 1994;50:7–15.

34. Fellows LK, Farah MJ. Different underlying impairments in decision-making following ventromedial and dorsolateral frontal lobe damage in humans. Cereb Cortex N Y N 1991. 2005;15:58–63.

35. Castrioto A, Funkiewiez A, Debû B, et al. Iowa gambling task impairment in Parkinson's disease can be normalised by reduction of dopaminergic medication after subthalamic stimulation. J Neurol Neurosurg Psychiatry. 2015;86:186–190.

36. Pineau F, Roze E, Lacomblez L, et al. Executive functioning and risk-taking behavior in Parkinson's disease patients with impulse control disorders. J Neural Transm Vienna Austria 1996. 2016;123:573–581.

37. Czernecki V, Pillon B, Houeto JL, Pochon JB, Levy R, Dubois B. Motivation, reward, and Parkinson's disease: influence of dopatherapy. Neuropsychologia. 2002;40:2257–2267.

38. Santangelo G, Raimo S, Barone P. The relationship between Impulse Control Disorders and cognitive dysfunctions in Parkinson's Disease: A meta-analysis. Neurosci Biobehav Rev. 2017;77:129–147.

39. Sebastian A, Pohl MF, Klöppel S, et al. Disentangling common and specific neural subprocesses of response inhibition. NeuroImage. 2013;64:601–615.

40. Jahfari S, Waldorp L, van den Wildenberg WPM, Scholte HS, Ridderinkhof KR, Forstmann BU. Effective connectivity reveals important roles for both the hyperdirect (fronto-subthalamic) and the indirect (fronto-striatal-pallidal) fronto-basal ganglia pathways during response inhibition. J Neurosci Off J Soc Neurosci. 2011;31:6891–6899.

41. Jahanshahi M, Obeso I, Baunez C, Alegre M, Krack P. Parkinson's Disease, the Subthalamic Nucleus, Inhibition, and Impulsivity: PD, The STN, Inhibition, and Impulsivity. Mov Disord. 2015;30:128–140.

42. Antonelli F, Ko JH, Miyasaki J, et al. Dopamine-agonists and impulsivity in Parkinson's disease: Impulsive choices vs. impulsive actions: Dopamine-Agonists and Impulsivity in PD. Hum Brain Mapp. 2014;35:2499–2506.

43. Verger A, Klesse E, Chawki MB, et al. Brain PET substrate of impulse control disorders in Parkinson's disease: A metabolic connectivity study. Hum Brain Mapp. Epub 2018 Apr 10.

44. Aron AR, Robbins TW, Poldrack RA. Inhibition and the right inferior frontal cortex. Trends Cogn Sci. 2004;8:170–177.

45. Ray NJ, Brittain J-S, Holland P, et al. The role of the subthalamic nucleus in response inhibition: Evidence from local field potential recordings in the human subthalamic nucleus. NeuroImage. 2012;60:271–278.

46. Alegre M, Lopez-Azcarate J, Obeso I, et al. The subthalamic nucleus is involved in successful inhibition in the stop-signal task: A local field potential study in Parkinson's disease. Exp Neurol. 2013;239:1–12.

47. Benis D, David O, Lachaux J-P, et al. Subthalamic nucleus activity dissociates proactive and reactive inhibition in patients with Parkinson's disease. NeuroImage. 2014;91:273–281.

48. Anzak A, Gaynor L, Beigi M, et al. Subthalamic nucleus gamma oscillations mediate a switch from automatic to controlled processing: a study of random number generation in Parkinson's disease. NeuroImage. 2013;64:284–289.

49. Anzak A, Gaynor L, Beigi M, et al. A gamma band specific role of the subthalamic nucleus in switching during verbal fluency tasks in Parkinson's disease. Exp Neurol. 2011;232:136–142.

50. Aron AR. Cortical and Subcortical Contributions to Stop Signal Response Inhibition: Role of the Subthalamic Nucleus. J Neurosci. 2006;26:2424–2433.

51. Aron AR, Behrens TE, Smith S, Frank MJ, Poldrack RA. Triangulating a Cognitive Control Network Using Diffusion-Weighted Magnetic Resonance Imaging (MRI) and Functional MRI. J Neurosci. 2007;27:3743–3752.

52. Rodriguez-Oroz MC, López-Azcárate J, Garcia-Garcia D, et al. Involvement of the subthalamic nucleus in impulse control disorders associated with Parkinson's disease. Brain. 2011;134:36–49.

53. Voon V, Pessiglione M, Brezing C, et al. Mechanisms underlying dopamine-mediated reward bias in compulsive behaviors. Neuron. 2010;65:135–142.

54. Piray P, Zeighami Y, Bahrami F, Eissa AM, Hewedi DH, Moustafa AA. Impulse Control Disorders in Parkinson's Disease Are Associated with Dysfunction in Stimulus Valuation But Not Action Valuation. J Neurosci. 2014;34:7814–7824.

55. Naqvi NH, Gaznick N, Tranel D, Bechara A. The insula: a critical neural substrate for craving and drug seeking under conflict and risk. Ann N Y Acad Sci. 2014;1316:53–70.

56. Xue G, Lu Z, Levin IP, Bechara A. The impact of prior risk experiences on subsequent risky decision-making: the role of the insula. NeuroImage. 2010;50:709–716.

57. Carriere N, Lopes R, Defebvre L, Delmaire C, Dujardin K. Impaired corticostriatal connectivity in impulse control disorders in Parkinson disease. Neurology. 2015;84:2116–2123.

58. Aron AR, Fletcher PC, Bullmore ET, Sahakian BJ, Robbins TW. Stop-signal inhibition disrupted by damage to right inferior frontal gyrus in humans. Nat Neurosci. 2003;6:115–116.

59. Sano H, Chiken S, Hikida T, Kobayashi K, Nambu A. Signals through the striatopallidal indirect pathway stop movements by phasic excitation in the substantia nigra. J Neurosci Off J Soc Neurosci. 2013;33:7583–7594.

60. Obeso I, Wilkinson L, Casabona E, et al. The subthalamic nucleus and inhibitory control: impact of subthalamotomy in Parkinson's disease. Brain. 2014;137:1470–1480.

SUPPLEMENTARY DATA

Classical and Modified Iowa Gambling Talks (IGT)

The classical IGT is a computerized measure that was originally developed to evaluate defective decision-making observed in patients with damage to the ventromedial prefrontal cortex (vmPFC)[1]. These patients often engaged in risky or impulsive behavior in their daily lives and seemed unable to learn from the consequences of their poor judgment, but performed normally on neuropsychological measures of executive function[1,2]. The IGT simulates a card game in which the player tries to win 'money' by choosing cards from four decks. Each deck contains cards that award money (positive rewards/feedback) but may also take money away (negative rewards/feedback). Two decks (A&B) are disadvantageous decks that provide large rewards but even larger punishments resulting in a net loss over time. Two other decks (C&D) are advantageous decks that provide small rewards but even smaller punishments resulting in a net gain over time. Examinees are told in advance that they must accrue as much 'money' as possible. The primary dependent variable is the number of advantageous minus disadvantageous selections in each block of 20 trials [(C + D) – (A + B)]. Successful performance in the IGT requires intact decision-making, reversal learning, impulse control, mental flexibility, and reward/punishment sensitivity[3–5]. Over time, the players ideally learn that choosing from the two advantageous decks will maximize their winnings. However, players with damage to the vmPFC typically persist in choosing from the disadvantageous decks which yield higher rewards even as their losses mount[1,2]. Bechara and colleagues referred to this neglect of future consequences and single-minded focus on desirable present outcomes as 'myopia for the future'[3,6]. In addition to the original clinical population of vmPFC patients, the IGT has also demonstrated sensitivity to poor decision-making skills in other patient groups with impulsive behaviors, including substance abuse patients and pathological gamblers. These non-lesion

groups are typically not as severely impaired and eventually develop some preference for the advantageous decks[7,8].

The modified IGT used in the scanner was a simplified version of the classical IGT designed to minimize motor difficulties experienced by PD patients during scanning and to assure that they could understand the IGT contingencies. Instead of the original version (with decks A, B, C and D), we used a version with only two decks (A and B). One of the decks was disadvantageous, providing larger gains but larger losses resulting in a net loss over time. The other deck was advantageous, providing smaller gains but smaller losses resulting in a net gain over time. These deck contingencies were kept consistent across conditions (i.e., positive, negative and mixed), regardless of the feedback specifically provided in each of these conditions. Similar to the classical IGT, participants were told in advance that they must accrue as much 'money' as possible. The primary dependent variable was the number of advantageous selections minus disadvantageous selections. The subject chose a card from either of the two decks, then a message was displayed on the screen indicating the amount of money the subject had won or lost. The task was divided into 3 conditions, always presented in the same sequential order: (1) only positive feedback was presented, so the participants could get familiarized with the decks providing lower and higher gains (positive); (2) negative feedback was presented, so participants could get familiarized with the decks providing higher and lower losses (negative); and, (3) positive and negative feedback was provided, so participants could either win or lose money based on the contingencies learned in sections 1 and 2. Participants performed this modified version of the IGT across three functional runs. Within each of these functional runs, participants performed two blocks, each including the three sequential sections (6 in total). Blocks presented within the same functional run differed from each other in regard to the advantageous/disadvantageous rules applied, and participants were instructed to ignore previous contingencies when moving from one block to the next. Between blocks participants performed a control task where they encountered two decks (A and B) with amounts displayed on top of the decks and just needed to choose the deck displaying the higher number. During this control

task the amounts that appeared in decks A and B were fully randomized and participants only needed to choose either deck based on the currently displayed amounts rather than on contingencies associated with the decks.

Statistical analyses of clinical data

SPSS v16.0 was used to perform statistical analyses on the demographic variables and the IGT performance. The distributions of demographic variables were tested for normality using the Shapiro-Wilk test. Sociodemographic differences between groups were tested with the Analysis of Variance (ANOVA) or Kruskal-Wallis test for 3-group comparisons and 2-tailed t-test or U-Mann Whitney for 2-group comparisons, respectively. IGT performance was analyzed in the conventional way by dividing the task into five blocks of 20 consecutive card selections. An ANOVA with repeated measures was performed using Group as between factor, Block as within factor and the Net score [(advantageous decks)-(disadvantageous decks)] as the dependent measure. For each statistic test, a two-tailed probability value of <0.05 was regarded as significant.

MRI data acquisition

Data were obtained at the Basque Center on Cognition, Brain and Language (BCBL) 3T Siemens Magnetom TIM Trio MRI scanner (Siemens Medical Solutions, Erlangen, Germany) using a 32-channel head coil. PD patients were under the effects of their usual dopaminergic medication during MRI scanning. Ear plugs and snugly-fitting headphones (MR Confon, Magdeburg, Germany) were used to dampen background scanner noise and to enable communication with experimenters while in the scanner. To limit head movement, the area between participants' heads and the coil was padded with foam and participants were asked to remain as still as possible.

Functional images were acquired in three separate runs using a gradient-echo echo-planar pulse sequence with the following acquisition parameters: TR = 2000 ms, time echo (TE) = 28 ms, 33 contiguous 3 mm^3 axial slices, 10% inter-slice gap, flip angle (FA) = 90º, field of view (FoV) = 192 x 192 mm. 320 volumes were collected per functional run. Prior to each scan, four volumes were discarded to allow for T1-Equilibration effects. Structural T1-weighted images were acquired with a MPRAGE sequence with TR = 2530 ms, TE = 2.97 ms, inversion time = 1100 ms, FA = 7°, FoV = 256x256 mm, 176 slices and voxel size = 1 mm^3.

MRI data analyses

SPM8 (Welcome Department of Cognitive Neurology, London) was used to conduct standard preprocessing routines and analyses. Images were corrected for differences in timing of slice acquisition and were realigned to the first volume by means of rigid-body transformation. Then, functional images were spatially smoothed using a 4-mm full width at half-maximum (FWHM) isotropic Gaussian kernel. Next, motion parameters obtained from realignment were used to inform a volume repair procedure (ArtRepair; Stanford Psychiatric Neuroimaging Laboratory) that identified bad volumes on the basis of within-scan movement and signal fluctuations, and then corrected bad signal values via interpolation. A volume-by-volume correction with a 0.5 mm threshold was applied, which did not correct more than 20% of the total volumes in any participant. Six additional subjects not included in the final sample described in the *participants* section above were excluded due to excessive motion with either more than 20% to-be-repaired functional volumes or drifts over 3 mm in any of the functional runs. After volume repair, structural and functional volumes were corregistered and spatially normalized to T1 and echo-planar imaging templates, respectively. The normalization algorithm used a 12-parameter affine transformation together with a non-linear transformation involving cosine basis functions. During normalization, the volumes were sampled to 3-mm cubic voxels. Templates were based on the MNI305 stereotaxic space. Then, functional volumes were spatially smoothed with a 7-

mm FWHM isotropic Gaussian kernel. Finally, a 128 sec high-pass filter was used to eliminate contamination from slow drift of signals.

Statistical analyses were performed on individual participants' data using the general linear model (GLM). The fMRI time series data were modeled by a series of events convolved with a canonical hemodynamic response function. Four fMRI task experimental conditions were analyzed separately as epochs from the onset of the presentation of the first stimulus within each section (positive feedback, negative feedback, mixed feedback) and control task. The resulting functions were used as covariates in a GLM, along with the motion parameters for translation (i.e., x, y, z) and rotation (i.e., yaw, pitch, roll) as covariates of non-interest. The model was created to examine the neural changes restricted to the three task sections and the control task periods and was used in whole-brain contrast, regions-of-interest (ROIs), time course and functional connectivity (FC) analyses.

The least-squares parameter estimates of the height of the best-fitting canonical HRF for each condition were used in pairwise contrasts. Contrast images, computed on a participant-by-participant basis were submitted to group analysis. At the group level, the whole-brain contrasts between the three main conditions and the control condition were computed by performing one-sample t-tests on these images, treating participants as a random effect. The standard statistical threshold for whole-brain map involving all participants and contrasting all the experimental conditions versus the control task (i.e., All Conditions > Control) was a voxel-wise corrected false discovery rate (FDR) set at $q < 0.01$. Brain coordinates in this manuscript are reported in Montreal Neurological Institute (MNI) atlas space[9].

ROI analyses were performed with the MARSBAR toolbox for use with SPM8[10]. ROIs consisted of significantly active voxels identified from the All Conditions > Control whole-brain contrast ($q < 0.01$, voxel-wise FDR corrected) across all participants within specific MARSBAR anatomical ROIs. A set of ROIs (the center of mass and the volume in cubic mm are indicated between parentheses) were built, including: left middle frontal gyrus (MFG) (-39, -

33, 32; 17760 mm^3), left orbitofrontal (OFC) (-38, 52, -7; 3024 mm^3), left insula (-35, 19, -2; 1256 mm^3), right MFG (38, 34, 32; 30208 mm^3), right supplementary motor area (SMA) (9, 20, 59; 2360 mm^3), right inferior frontal gyrus (IFG) (46, 25, 9; 11864 mm^3), right insula (38, 20, -3; 2824 mm^3), right subthalamic nucleus (STN) (15, -13, -4; 162 mm^3) and right ventral striatum (VS) (21, 10, -7; 3944 mm^3). One-way analysis of variance (ANOVA) followed by Scheffé post-hoc analyses were used to compare results among groups in each ROI.

We also performed time-course analyses for the fMRI trials. Blood Oxygen Level Dependent (BOLD) activity time series, averaged across all voxels in each ROI, were extracted for each functional run. Mean time courses for each trial were then constructed by averaging together appropriate trial time courses per condition, which were defined as 16 sec windows of activity after trial onset. In detail, these 16 seconds were divided into two periods: an initial period from 0 to 8 seconds and a final period from 8 to 16 seconds. These condition-averaged time courses were then averaged across functional sessions and across participants. For each ROI, we performed a mixed-model ANOVA on the BOLD signal intensity with the factors Group (PD-ICD, PD-noICD, HC), Condition (positive feedback, negative feedback, mixed feedback), and Time (initial period, final period).

To examine associations between regional hyperactivation and ICD severity in PD-ICD patients, we conducted one-tailed Pearson correlation analyses between the percentage signal change observed in the previously mentioned regions of interest and the QUIP-RS scores, correcting for multiple comparisons ($q < 0.05$, FDR).

We assessed FC via the beta series correlation method[11] implemented in SPM8 with custom Matlab scripts. The canonical HRF in SPM was fit to each occurrence of each condition and the resulting parameter estimates (beta values) were sorted according to the study conditions of interest to produce a condition-specific beta series for each voxel. Pairwise FC analyses were conducted for the negative feedback condition calculating the beta-series correlation values for each pair of right-lateralized ROIs that showed significant positive associations with ICD

severity in the PD-ICD group (i.e., STN, VS, insula, IFG, SMA, and MFG). Since the correlation coefficient is inherently restricted to range from −1 to +1, an arc-hyperbolic tangent transform[12] was applied to these beta-series correlation values (r values) to make its null hypothesis sampling distribution approach that of the normal distribution. To examine associations between FC among these six ROIs and ICD severity, we conducted two-tailed Pearson correlation analyses between Fisher z-score transformed beta-series correlation values and the QUIP-RS scores, correcting for multiple comparisons ($q < 0.05$, FDR).

Finally, mediation analyses were conducted to examine whether in PD-ICD patients pairwise FC between nodes (i.e., right-lateralized STN-VS, VS-IFG and VS-Insula) during the negative feedback condition mediates the relation between ICD severity and regional functional activation of areas critically involved in conflict detection and inhibitory control processes. To this end, we followed the four steps described by Baron and Kenny to establish mediation[13]. A significant mediator was indicated when the relationship between the ICD severity (QUIP-RS) and local signal intensity is no longer significant after controlling for the mediator.

Supplementary Figure 1. IGT performance over time in PD-ICD, PD-noICD and HC groups. The result is the difference between the percentage of advantageous choices minus the percentage of disadvantageous choices.

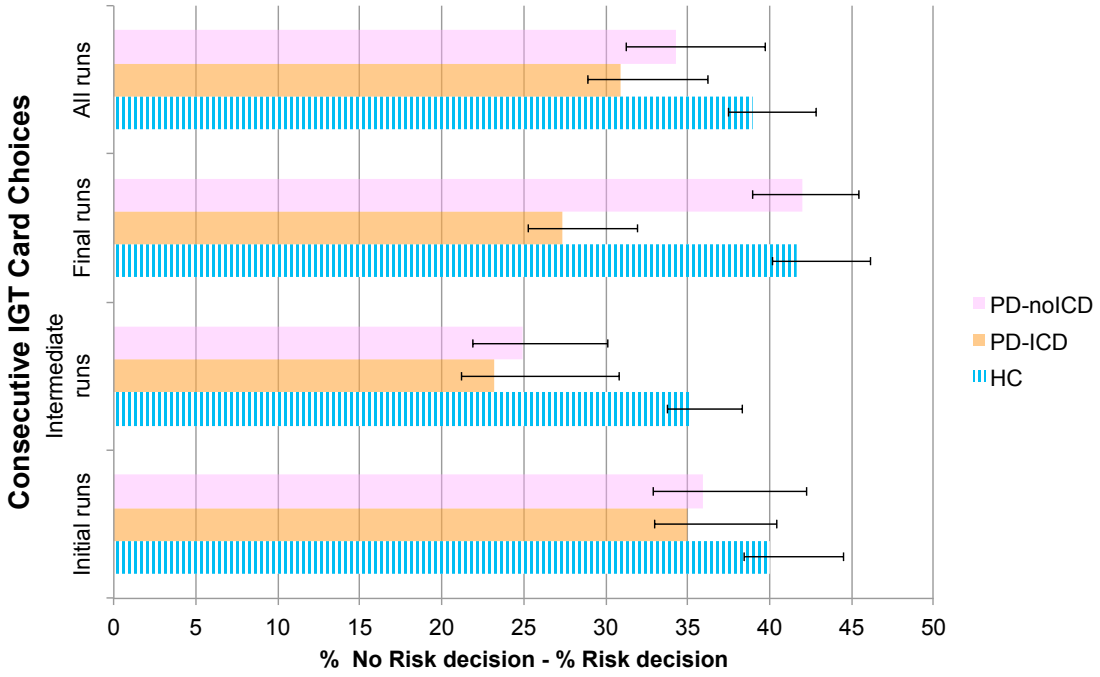

As in the IGT task performed during the neuropsychological investigations, no significant differences were found between groups. The ANOVA on the net scores revealed no significant main effects of Group (F (2, 50) = 0.19; p = 0.82, η_p^2 = 0.08) nor Group by Condition by Run interaction (F (4, 50) = 0.78; p = 0.54, η_p^2 = 0.03) or other interaction between factors.

REFERENCES

1. Bechara A, Damasio AR, Damasio H, Anderson SW. Insensitivity to future consequences following damage to human prefrontal cortex. Cognition. 1994;50:7–15.

2. Bechara A, Tranel D, Damasio H, Damasio AR. Failure to respond autonomically to anticipated future outcomes following damage to prefrontal cortex. Cereb Cortex. 1996;6:215–225.

3. Fellows LK, Farah MJ. Different underlying impairments in decision-making following ventromedial and dorsolateral frontal lobe damage in humans. Cereb Cortex. 2005;15:58–63.

4. Mimura M, Oeda R, Kawamura M. Impaired decision-making in Parkinson's disease. Parkinsonism Relat Disord. 2006;12:169–175.

5. Thiel A, Hilker R, Kessler J, Habedank B, Herholz K, Heiss W-D. Activation of basal ganglia loops in idiopathic Parkinson's disease: a PET study. J Neural Transm (Vienna). 2003;110:1289–1301.

6. Bechara A, Tranel D, Damasio H. Characterization of the decision-making deficit of patients with ventromedial prefrontal cortex lesions. Brain. 2000;123 (Pt 11):2189–2202.

7. Goudriaan AE, Oosterlaan J, de Beurs E, van den Brink W. Decision making in pathological gambling: a comparison between pathological gamblers, alcohol dependents, persons with Tourette syndrome, and normal controls. Brain Res Cogn Brain Res. 2005;23:137–151.

8. Rossi M, Gerschcovich ER, Gerschcovich ER, et al. Decision-making in Parkinson's disease patients with and without pathological gambling. Eur J Neurol. 2010;17:97–102.

9. Cocosco CA, Kollokian V, Kwan RKS, Evans AC. Brainweb: online interface to a 3D MRI simulated brain database. Neuroimage Proc HBM´97. 1997;5 (4):S425.

10. Brett, M., Anton, J.-L., Valabregue, R. and Poline, J.-B. Region of Interest Analysis Using the MarsBar Toolbox for SPM 99. NeuroImage. 16:497.

11. Rissman J, Gazzaley A, D'Esposito M. Measuring functional connectivity during distinct stages of a cognitive task. Neuroimage. 2004;23:752–763.

12. Fisher RA. On the "probable error" of a coefficient of correlation deduced from a small sample. Metron. 1921;1:3–32.

13. Baron RM, Kenny DA. The moderator-mediator variable distinction in social psychological research: conceptual, strategic, and statistical considerations. J Pers Soc Psychol. 1986;51:1173–1182.

Supplementary Table 1. Neuropsychological test scores of the sample.

	PD-ICD n=18	**PD-noICD n=17**	**HC n=18**	***p***
MoCA	27 (2.2)	27.3 (3)	28 (1.7)	0.444[a]
Digit span *forward*	6 [5-6.7]	6 [4.6-7.2]	7 [6.2-7.1]	0.134[b]
Digit span *backwards*	4 [3.9-5.6]	4 [3.1-5.7]	5 [4.2-6.5]	0.117[b]
TMT-A (s)	46.35 [23.4-54.1]	39.8 [25.5-46.2]	34.5 [22.2-45.3]	0.418[b]
TMT-B (s)	88.5 [63.3-118.7]	82.2 [61.4-95.8]	71.2 [59-95.4]	0.493[b]
Stroop words	96.1 (18.2)	93 (26.3)	106.6 (21.5)	0.180[a]
Stroop colors	60.9 (14.8)	59.2 (19.4)	69.2 (14.9)	0.174[a]
Stroop words-colors	33.4 (11.8)	34 (13.1)	41 (12)	0.135[a]
Phonemic fluency (initial letter)	16.1 (5.5)	14.4 (5.4)	18.2 (5.7)	0.112[a]
LNS	11.1 [8.5-11.3]	10 [8.2-11.1]	11.6 [11-2-13.7]	0.333[b]
RAVLT total recall	46.3 (7.8)	47.7 (16.1)	50.7 (9.8)	0.228[a]
RAVLT delayed recall	9.1 (2.9)	8.6 (4.7)	9.7 (3.6)	0.103[a]
RAVLT recognition	14 [11.8-15.2]	12 [7-14.3]	14.2 [13.5-15.6]	0.378[b]
Semantic fluency (animals)	21.5 (5.6)	20 (7.6)	23.1 (4.8)	0.328[a]
Boston naming test	12 [9.8-13.2]	13 [10.7-14.5]	13.5 [12.4-15.8]	0.416[b]
VOSP Object decision	16.8 (2.1)	16 (4.5)	17.5 (2.1)	0.517[a]
VOSP Number location	9.7 (0.6)	8.4 (2.5)	9.8 (0.8)	0.125[a]

The data are given as absolute values, mean (SD), median (IQR) or n (%): [a]ANOVA-one factor; [b]Kruskal-Wallis test.

Abbreviations: MoCA, Montreal Cognitive Assessment; TMTA, part A of Trail Making Test; TMTB, part B of Trail Making Test; LNS, Letters and Number Sequencing; RAVLT, Rey Auditory Verbal Learning Test; VOSP, Visual Object and Space Perception Battery

Supplementary Table 2 Characteristics of ICD in PD patients.

SUBJECTS	SEX (M/F)	AGE (years)	MAIN ICD	Other ICDs	DA
PD-ICD 1	M	64	BE	Hobbysm	Pramipexole
PD-ICD 2	M	64	HS	-	Pramipexole

PD-ICD 3	M	59	BE	-	Pramipexole
PD-ICD 4	F	64	CS	Hobbysm	Pramipexole
PD-ICD 5	M	65	BE	CS, hobbysm	Ropinirole
PD-ICD 6	M	61	CS	Hobbysm	Rotigotine
PD-ICD 7	M	48	HS	-	-
PD-ICD 8	M	68	HS	BE	Pramipexole
PD-ICD 9	M	57	PG	BE	Pramipexole
PD-ICD 10	M	44	BE	Hobbysm	Rotigotine
PD-ICD 11	M	61	BE	-	Pramipexole
PD-ICD 12	M	58	BE	Hobbysm	Apomorphine sc
PD-ICD 13	M	71	HS	CS, BE	Rotigotine
PD-ICD 14	M	75	HS	-	Rotigotine
PD-ICD 15	M	68	HS, CS	Hobbysm, Punding	Ropinirole
PD-ICD 16	M	65	HS	BE	Pramipexole
PD-ICD 17	M	60	CS	HS, BE, Punding	Rotigotine
PD-ICD 18	F	69	BE	-	Rotigotine

M = male; F = female; BE = binge eating; HS = hypersexuality; CS = compulsive shopping; PG = pathological gambling; DA = dopamine agonist. All patients were also taking levodopa.